

Influence of flexoelectricity above the nematic Fréedericksz transition

C. V. Brown¹ and N. J. Mottram²

¹*Physics and Mathematical Sciences, The Nottingham Trent University, Clifton Lane, Nottingham NG11 8NS, United Kingdom*

²*Department of Mathematics, University of Strathclyde, Glasgow G1 1XH, United Kingdom*

(Received 17 January 2003; published 5 September 2003)

Continuum theory is used to demonstrate that the presence of flexoelectricity significantly alters the response to an applied voltage of a homogeneous nematic liquid crystal cell above the ac Fréedericksz threshold voltage. In such a system there is a fitting degeneracy: we obtain very good fits between theory and experimental permittivity data using any value of the sum of flexoelectric coefficients, $e_{11} + e_{33}$, between 0.0 C/m and 1.5×10^{-11} C/m. The corresponding values of the nematic bend elastic constant show an inverse parabolic relationship with $e_{11} + e_{33}$, with K_{33} being reduced down to 90% of its value when flexoelectricity is neglected.

DOI: 10.1103/PhysRevE.68.031702

PACS number(s): 42.70.Df, 61.30.Dk, 61.30.Eb, 77.84.Nh

I. INTRODUCTION

In the continuum theory of Frank [1] and Oseen [2] the magnitude of the splay, twist, and bend elastic distortions in a nematic liquid crystal director field are parametrized by the K_{11} , K_{22} , and K_{33} elastic constants, respectively. Knowledge of these parameters has played a critical role in the exploitation of liquid crystals for the development of what have proved to be highly successful commercial display devices.

The standard approach to increasing the speed, contrast, and brightness of conventional liquid crystal displays has involved the development of nematic liquid crystal mixtures possessing elastic and dielectric material properties which have been specifically tailored for the particular type of display. This development process has relied on the ability to accurately measure these material properties which, over the last 20 years, has enabled the fundamental relationships between the bulk properties and the microscopic molecular ordering and intermolecular interactions in the nematic phase to be investigated [3–6].

Measurement of nematic elastic constants is generally carried out using a relatively simple liquid crystal cell geometry, chosen so that the orienting torque due to an applied electric field is in competition with the elastic torque exerted by the cell boundaries. The ac Fréedericksz effect [3,7], that is based on this principle, has been used as a standard technique to determine the values of the K_{11} and K_{33} elastic constants. In this method the director reorientation in the bulk of the liquid crystal layer starts to occur only when the applied ac voltage is above a critical value, the Fréedericksz threshold.

In this paper the influence of an additional material property, the flexoelectric polarization, when using the ac Fréedericksz technique is investigated. Meyer [8] proposed that an ensemble of nematic molecules that possess a shape polarity as well as a permanent electric dipole moment will also show a flexoelectric effect, in analogy to the piezoelectric effect in crystals. For these nematic materials a splay or bend deformation will induce a polarization in the material

$$\mathbf{P} = e_{11} \mathbf{n}(\nabla \cdot \mathbf{n}) + e_{33}(\nabla \times \mathbf{n}) \times \mathbf{n}, \quad (1)$$

where \mathbf{n} is the nematic director, a unit vector which denotes the locally averaged molecular orientation, and the flexoelectric coefficients e_{11} and e_{33} in Eq. (1) correspond to splay and bend distortions, respectively. The existence of this effect has since been verified for a number of different nematic and cholesteric materials, both polar and nonpolar, although the values obtained for the nematic flexoelectric coefficients measured using different techniques have shown large discrepancies in certain materials [9–13].

In previous work the influence of the flexoelectric polarization on the magnetic Fréedericksz effect has been considered [14]. Small changes were observed in the retardation of the liquid crystal layer above the threshold field as the sweep rate of the magnetic field was changed. The magnitude of these changes gave an estimate of the value of e_{11} and e_{33} . In the current work a detailed theoretical study has been undertaken to investigate the effect that a finite flexoelectric polarization will have on the electric field response of a homogeneous nematic liquid crystal cell above the ac Fréedericksz threshold voltage.

II. THE FRÉEDERICKSZ EFFECT

The geometry that will be considered in this paper comprises a nematic liquid crystal layer sandwiched between two conducting electrodes in which the average molecular alignment, or director, is parallel to the bounding plates at all points in the layer. In the analysis that follows it will be assumed that the liquid crystal molecules at the bounding plate are rigidly aligned in a direction that is exactly parallel to the plates.

In Fig. 1 the filled circles show experimental measurements of the permittivity for a Fréedericksz cell of thickness 5.5×10^{-6} m filled with the nematic material *E7*, as a function of the rms of the applied ac voltage at a frequency of 2.0×10^3 Hz. This frequency was chosen to be large enough so that the liquid crystal shows a nonzero average response. The aligning agent on the cell surfaces was a rubbed polymer that gave a surface pretilt, the angle between the director and the cell surface, below 0.5° .

The data shows a very well-defined Fréedericksz threshold at $V_{rms} = 0.92$ V. Below this threshold there is no distortion of the liquid crystal director field which remains parallel

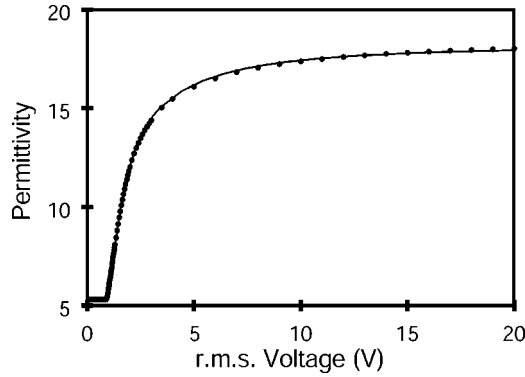


FIG. 1. Filled circles denote experimental data taken on a homogeneous Fréedericksz cell of thickness $5.5 \mu\text{m}$ filled with the material *E7* for applied ac voltages at a frequency of $2.0 \times 10^3 \text{ Hz}$. The solid line indicates the numerical fit to Eq. (2) with the parameters given in main text and with $e_{11} + e_{33} = 0.0 \text{ C/m}$.

to the substrates throughout the layer. The permittivity measured in this subcritical region corresponds to the permittivity perpendicular to the molecular director ϵ_{\perp} . Just above the threshold, the director starts to reorient in the bulk of the liquid crystal from the cell surface alignment direction towards the direction of the electric field. As the voltage is increased a greater proportion of the bulk region aligns with the field and so the permittivity asymptotes towards the value parallel to the molecular director ϵ_{\parallel} .

Continuum theory can be used to model the nematic liquid crystal and its interaction with the applied electric field and the critical rms voltage is found to be $V_c = \pi \sqrt{K_{11}/\epsilon_0 \Delta \epsilon}$, a function of the splay elastic constant K_{11} , the permittivity of free space ϵ_0 , and the dielectric anisotropy $\Delta \epsilon = \epsilon_{\parallel} - \epsilon_{\perp}$ [15]. Immediately above the threshold, and in the absence of any flexoelectric polarization, the field-induced reorientation of the nematic liquid crystal is predicted by continuum theory to be determined by the ratio of the elastic constants K_{33}/K_{11} [16].

III. THEORY

When the presence of flexoelectricity is included and we assume that fluid flow is of secondary importance, the governing equation for the director $\mathbf{n} = (\cos[\theta(z,t)], 0, \sin[\theta(z,t)])$ is given by the Ericksen-Leslie equation [17,18]

$$\begin{aligned} \gamma_1 \frac{\partial \theta}{\partial t} &= (K_{11} \cos^2 \theta + K_{33} \sin^2 \theta) \frac{\partial^2 \theta}{\partial z^2} \\ &+ (K_{33} - K_{11}) \sin \theta \cos \theta \left(\frac{\partial \theta}{\partial z} \right)^2 \\ &+ \epsilon_0 \Delta \epsilon E^2 \sin \theta \cos \theta - (e_{11} + e_{33}) \sin \theta \cos \theta \frac{\partial E}{\partial z}, \end{aligned} \quad (2)$$

where the rotational viscosity $\gamma_1 = \alpha_3 - \alpha_2$ is the difference between two Leslie viscosities and we have taken the z coordinate direction as the direction through the liquid crystal

layer, perpendicular to the cell surfaces. The electric field $E(z,t)$ is calculated, using Maxwell's equations, as $E(z,t) = (D_3 - P_3)/\epsilon_0(\epsilon_{\perp} + \Delta \epsilon \sin^2 \theta)$ in terms of, P_3 , the z component of the polarization vector given by Eq. (1) and the z component of the displacement field

$$D_3(t) = \frac{-(V_d - V_0) + \int_0^d \frac{(e_{11} + e_{33}) \sin(2\theta)}{\epsilon_0(\epsilon_{\perp} + \Delta \epsilon \sin^2 \theta)} \frac{\partial \theta}{\partial z} dz}{\int_0^d \frac{1}{\epsilon_0(\epsilon_{\perp} + \Delta \epsilon \sin^2 \theta)} dz}, \quad (3)$$

where $V_d - V_0$ is the potential difference between the cell electrodes. When the director is rigidly fixed at the two substrates, the flexoelectric contribution to D_3 , the second term in the numerator of Eq. (3), will integrate to zero. In the present case, a sinusoidal voltage of frequency f given by $V_d = \sqrt{2} V_{rms} \sin(2\pi ft)$ is applied at one electrode (at $z=d$, the cell thickness) with the other electrode (at $z=0$) at earth potential $V_0=0$. At both cell surfaces it is assumed that the director angle will take a fixed value so that $\theta(0,t) = \alpha$ and $\theta(d,t) = \alpha$ where α is the small pretilt angle, assumed to be zero in the analysis below.

Although we will later fit the experimental data to an exact numerical solution of Eq. (2), it is possible to obtain an approximate analytic solution and learn a great deal about the dynamical behavior of the director and electric field within the cell. If we assume that the rms applied voltage is only slightly above the critical voltage then the director angle within the cell will remain small and a perturbation approach may be used [19]. The director angle will then be the sum of a time-independent contribution, resulting from the response of the nematic to the root mean squared of the applied voltage, and a small oscillatory contribution from the high frequency ac voltage, $\theta(z,t) = \theta_0(z) + \theta_1(z,t)$. The electric field will consist of the applied ac field plus a small perturbation to this field, $E(z,t) = -(\sqrt{2} V_{rms}/d) \sin(2\pi ft) + E_1(z,t)$. Substituting these expressions into Eq. (1) and the calculation of the electric field leads to approximate expressions for the director angle and electric field

$$\theta(z,t) = \theta_m \sin\left(\frac{\pi z}{d}\right) - \frac{\theta_m \pi K_{11}}{4f \gamma_1 d^2} \sin\left(\frac{\pi z}{d}\right) \sin(4\pi ft), \quad (4)$$

$$\begin{aligned} E(z,t) &= -\frac{\sqrt{2} V_{rms}}{d} \sin(2\pi ft) - \frac{(e_{11} + e_{33}) \pi \theta_m^2}{2d \epsilon_0 \epsilon_{\perp}} \sin\left(\frac{2\pi z}{d}\right) \\ &- \frac{\pi \theta_m^2 \sqrt{\Delta \epsilon K_{11}}}{d \epsilon_{\perp} \sqrt{2 \epsilon_0}} \cos\left(\frac{2\pi z}{d}\right) \sin(2\pi ft), \end{aligned} \quad (5)$$

where θ_m is the maximum distortion in the middle of the cell.

Equation (4) is the expected form of the director response to a high frequency ac voltage: a time-periodic perturbation, at a frequency that is double that of the applied voltage, and a time-independent director angle offset. Since f has been assumed to be large, the second term in Eq. (4) is consider-

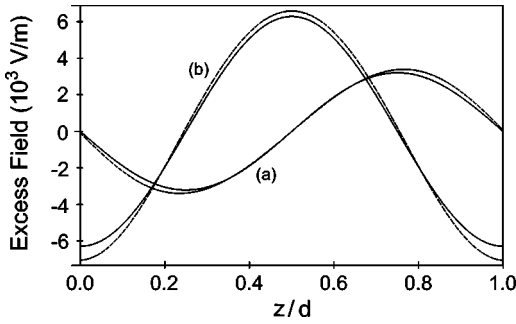


FIG. 2. (a) The numerically (dashed lines) and analytically (solid lines) calculated time averaged excess electric field as a function of the distance z/d through the cell. (b) The numerically (dashed lines) and analytically (solid lines) calculated ac component of the excess electric field as a function of the distance z/d through the cell.

ably smaller in magnitude than the first term. The only difference in the director angle when flexoelectricity is present is that the magnitude of the director response θ_m is altered.

However, the form of the electric field in Eq. (5) has an important dependency on the flexoelectric coefficients. We see that there exists a dc contribution in the electric field solution, the second term in Eq. (5), which would disappear if flexoelectricity was ignored. This dc contribution is antisymmetric within the cell, that is, the dc component in one-half of the cell is exactly the negative of that in the other half of the cell.

Figures 2 and 3 illustrate the electric field solution in Eq. (5) as well as the numerical solution to Eqs. (2) and (3) with the parameters $K_{11}=1.01621 \times 10^{-11}$ N, $K_{33}=1.63508 \times 10^{-11}$ N, $\epsilon_{\parallel}=18.6454$, $\epsilon_{\perp}=5.3064$, $V_{rms}=0.94$ V, $f=1000$ Hz, and with the flexoelectric coefficients $e_{11}+e_{33}=2.5 \times 10^{-11}$ C/m. For this voltage, close to the transition voltage of 0.92 V, there is only a small director deflection in the middle of the cell of $\theta_m=8.322^\circ$ and the approximate analytical solution is in good agreement.

In Fig. 2(a) the numerically calculated excess electric field (dashed lines), which is the total electric field in the cell minus the applied electric field, has been integrated over one time period of the applied field and compared to the second term in the analytic solution (solid lines) in Eq. (5). The

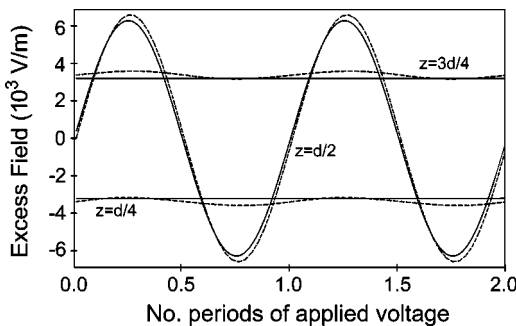


FIG. 3. The excess electric field in the middle of the cell, $z=d/2$, and at the points $z=d/4$ and $3d/4$. Solid curves are plots of the analytic solution in Eq. (5) and the dashed lines denote the numerical solution to Eqs. (2) and (3).

numerically calculated dc excess field component is clearly in good agreement with the analytic solution, for which we have used the value $\theta_m=8.322^\circ$. The antisymmetry of the dc component is clearly seen and shows that the dc field value at the center of the cell is zero. Figure 2(b) shows the numerically calculated ac component of the excess field, the excess field minus the dc component, at a quarter period ($t=1/4f$). The numerical and analytic solutions are again in good agreement. Figure 3 shows the numerical (dashed lines) and analytical (solid lines) excess electric field solutions as a function of time over two periods of the applied electric field. It is clear from this figure that the dc component is zero at the center of the cell, $z=d/2$, leaving only the oscillating ac component. At the quarter points in the cell, $z=d/4$ and $z=3d/4$, the dc component is nonzero but the ac component is small. In fact in the ideal analytic solution the ac component, the third term in Eq. (5), is exactly zero at the points $z=d/4$ and $z=3d/4$.

As discussed below, the presence of a dc component of the electric field, even when the applied electric field is oscillatory, will significantly affect any ions within the cell. This flexoelectricity-induced dc component also couples to the director distortion leading to a change in the effective permittivity.

IV. FITTING THE EXPERIMENTAL DATA

A very good fit between experimental data and the numerical solution may be obtained. The solid line in Fig. 1 shows a theoretical fit to the Fréedericksz curve using the exact numerical solution of Eq. (2) with the parameters given in Sec. III and for which the sum of the flexoelectric coefficients, $e_{11}+e_{33}$, has been set to zero. For both the experimental data and the numerical solution of the equation, a sinusoidal voltage of frequency f given by $V_d=\sqrt{2}V_{rms}\sin(2\pi ft)$ is applied across the cell. The experimentally measured permittivity is then found theoretically by calculating the ratio of the time differential of the displacement field dD_3/dt to applied voltage $V_d(t)$. This analysis assumes that the cell is operating in the linear response regime in which the output displacement field is also sinusoidal as a function of time. This assumption is correct for the material E7 at the frequency used, $f=2.0 \times 10^3$ Hz.

Just above the threshold region critical slowing down occurs and so it must be ensured that sufficient time is allowed in both the simulation and the experimental measurement for equilibrium to be obtained. In addition, the density of experimental data is highly concentrated near to the threshold to weight the fit to that region which increases the accuracy with which K_{33}/K_{11} can be extracted.

The effect of a nonzero value of $e_{11}+e_{33}$ on the distorted director profile for applied voltages above the Fréedericksz transition voltage of 0.92 V is shown in Fig. 4. The solid lines were generated using Eq. (2) with $e_{11}+e_{33}=0$ C/m and for the dashed lines $e_{11}+e_{33}=2.5 \times 10^{-11}$ C/m. The value of the tilt angle in the center of the cell, θ_m , is larger for the higher applied voltage of 2.0 V as expected. However, for both applied voltages of 1.5 V and 2.0 V there is a reduction of θ_m when $e_{11}+e_{33}$ takes on the nonzero value. The reduc-

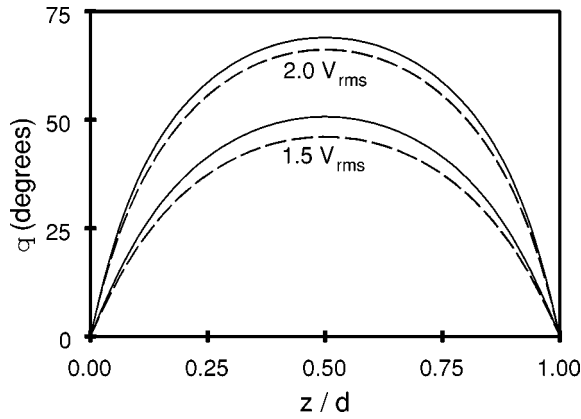


FIG. 4. Theoretical director profiles showing the effect of a nonzero value of $e_{11} + e_{33}$. The solid lines were generated using Eq. (2) with $e_{11} + e_{33} = 0$ C/m and for the dashed lines $e_{11} + e_{33} = 2.5 \times 10^{-11}$ C/m.

tion of θ_m when there is a nonzero flexoelectric polarization will be accompanied by a reduction in the value of the permittivity above the Fréedericksz threshold. However, both the exact numerical solution to Eq. (2) and the perturbation analysis predict that the threshold will still be given by $V_c = \pi \sqrt{K_{11} / \epsilon_0 \Delta \epsilon}$ and that V_c has no dependence on the value of $e_{11} + e_{33}$.

In Fig. 5 the lower curve is a repeat of the theoretical fit (solid line) to the data (filled circles) shown in Fig. 1 but here an expanded scale has been used. The curves shown above have been generated with nonzero values of the flexoelectric coefficients. Each curve has been shifted up by one unit and is shown with a repeat of the experimental data for clarity. The value of $e_{11} + e_{33}$ increases from 0.0 C/m (lower curve) in steps of 5.0×10^{-12} C/m to 2.5×10^{-11} C/m (upper curve). The values of $e_{11} + e_{33}$ that were used are comparable with the range of measured values reported for a number of different materials in the literature. In order to obtain the fit to the experimental data for the higher values of $e_{11} + e_{33}$ the

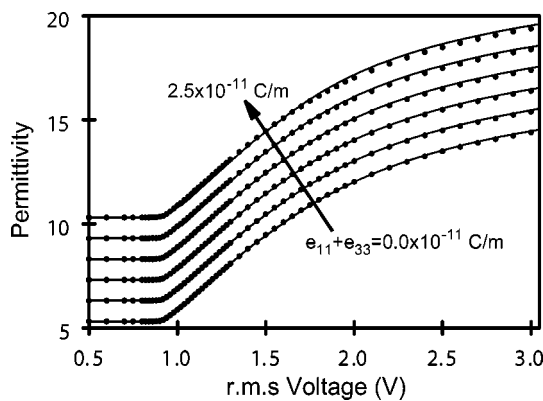


FIG. 5. Solid lines show theoretical curves generated for values of $e_{11} + e_{33}$ increasing from 0 C/m (lower) in steps of 5.0×10^{-12} C/m to 2.5×10^{-11} C/m (upper). In order to prevent the curves overlapping, each theoretical curve is displaced upwards by an additional 1.0 unit and the experimental data (filled circles) are repeated in the displaced positions.

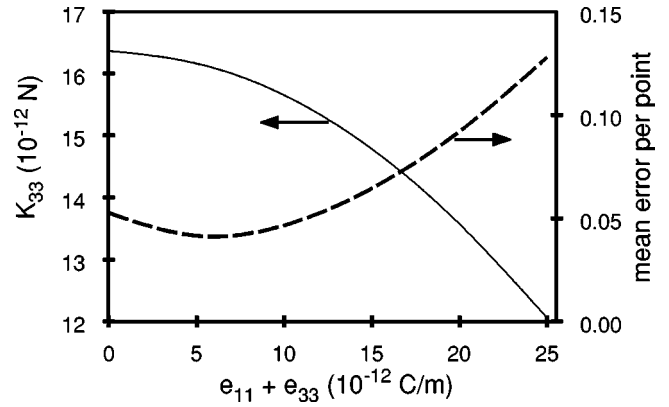


FIG. 6. The solid line shows the values of K_{33} and $e_{11} + e_{33}$ that give the best fit to the experimental data over the range 0.0–3.0 V shown in Fig. 3. The dashed line plots the average absolute difference between the theoretical curve and the experimental data as a function of $e_{11} + e_{33}$.

value of the K_{33} elastic constant has been decreased. For instance, for the highest value of $e_{11} + e_{33} = 2.5 \times 10^{-11}$ C/m the best fit was obtained with $K_{33} = 1.2045 \times 10^{-11}$ N, which has been reduced to 74% of the value calculated when the flexoelectric coefficients were set to zero. However, it is also qualitatively evident from Fig. 5 that the fit to the data has become poorer at the higher values of $e_{11} + e_{33}$.

It was found that small changes in the cell thickness had no effect on the shapes of the theoretical curves produced. It should also be noted that when the theoretical curves at the different values of $e_{11} + e_{33}$ are plotted on the expanded scale of Fig. 1 it is difficult to distinguish between them.

The solid line in Fig. 6 shows the relationship between the value of $e_{11} + e_{33}$ and of K_{33} that gave the best fits to the experimental data in the vicinity of the threshold region shown in Fig. 4. At the lower values of $e_{11} + e_{33}$ the change in K_{33} is relatively small, but the gradient of the curve increases for higher values. Here the exact numerical solution to Eq. (2) has been used to fit the data in the region up to three times the critical voltage.

The dashed line in Fig. 6 shows the mean absolute difference between the data and the theoretical curve, a quantitative measure of the quality of the fit to the experimental data. The quality of fit is very good for values below $e_{11} + e_{33} = 1.5 \times 10^{-11}$ C/m but above this value the mean error increases rapidly. This is consistent with the qualitative observation from Fig. 5. The minimum in the error that occurs in Fig. 6 cannot be regarded as an estimate of the true value of $e_{11} + e_{33}$ because the minimum is shallow and is therefore very sensitive to experimental variations in the region immediately above the threshold.

V. DISCUSSION AND CONCLUSION

It can be concluded that the value of the flexoelectric coefficient could lie within the range $e_{11} + e_{33} = 0.0$ C/m– 1.5×10^{-11} C/m and still be consistent with the measurements of the ac Fréedericksz transition. This obser-

vation could have serious implications for the standard measurement method for K_{33} and the subsequent use of the values in the modeling and optimization of liquid crystal devices.

The value of $e_{11} + e_{33}$ that has been measured using fully leaky guided mode techniques in Ref. [20] was 1.5×10^{-11} C/m, which falls within this range. However, the degeneracy in fitting the data between the value of K_{33} and the value of $e_{11} + e_{33}$ also applied to these measurements. It should also be noted that if there is any appreciable ionic contamination in the nematic material then this could have a screening effect on the flexoelectric polarization in a manner which is analogous to the possible ionic screening of the spontaneous polarization in ferroelectric liquid crystal materials [14,21,22]. In Ref. [22] it was predicted that the renormalization of the smectic- C^* bend elastic constants B_1 was directly influenced by the ionic screening length in the material.

In addition, we have shown that in the flexoelectric case the dc offset electric field is antisymmetric within the cell

and may therefore cause a drift of positive and negative ions towards the center of the cell and the cell boundaries, respectively (or vice versa depending on the sign of $e_{11} + e_{33}$).

The effects of a finite anchoring or of a finite pretilt have not been considered in the current work. If the anchoring was weak this leads to a systematic increase in the permittivity below the critical voltage and a less distinct transition at the threshold voltage. A finite pretilt above a certain value would have led to a number of different alignment configurations in the device [23]. Neither of these effects were observed in the current experimental cell. A theoretical treatment of the effects of flexoelectricity for cells with higher pretilt and containing ions will be addressed in a future publication.

ACKNOWLEDGMENTS

The authors gratefully thank J. S. Strömer and acknowledge Merck Chemicals Ltd. NB-C UK for the provision of the experimental data shown in Fig. 1, and Professor E. P. Raynes for many illuminating discussions.

-
- [1] F.C. Frank, *Discuss. Faraday Soc.* **25**, 19 (1958).
 - [2] C.W. Oseen, *Trans. Faraday Soc.* **29**, 883 (1933).
 - [3] M.J. Bradshaw and E.P. Raynes, *Mol. Cryst. Liq. Cryst.* **72**, 35 (1981).
 - [4] P.R. Gerber and M. Schadt, *Z. Naturforsch. A* **35A**, 1036 (1980).
 - [5] F.M. Leslie and C.M. Waters, *Mol. Cryst. Liq. Cryst.* **123**, 101 (1985).
 - [6] M.J. Bradshaw, E.P. Raynes, I. Fedak, and A.J. Leadbetter, *J. Phys. (Paris)* **45**, 157 (1984).
 - [7] V. Fréedericksz and V. Zolina, *Trans. Faraday Soc.* **29**, 919 (1933).
 - [8] R.B. Meyer, *Phys. Rev. Lett.* **22**, 918 (1969).
 - [9] J. Prost and P.S. Pershan, *J. Appl. Phys.* **47**, 2298 (1976).
 - [10] I. Dozov, P. Martinot-Lagarde, and G. Durand, *J. Phys. (Paris) Lett.* **43**, L365 (1982).
 - [11] N.V. Madhusudana and G. Durand, *J. Phys. (Paris) Lett.* **46**, L195 (1985).
 - [12] B. Valenti, C. Bertoni, G. Barbero, P. Taverna-Valabrega, and R. Bartolino, *Mol. Cryst. Liq. Cryst.* **146**, 307 (1987).
 - [13] L.M. Blinov, G. Durand, and S.V. Yablonsky, *J. Phys. II* **2**, 1287 (1992).
 - [14] H.J. Deuling, *Solid State Commun.* **14**, 1073 (1974).
 - [15] H. Gruler and G. Meier, *Mol. Cryst. Liq. Cryst.* **16**, 299 (1972).
 - [16] E.P. Raynes, R.J.A. Tough, and K.A. Davies, *Mol. Cryst. Liq. Cryst.* **56**, 63 (1979).
 - [17] J.L. Ericksen, *Arch. Ration. Mech. Anal.* **4**, 231 (1960).
 - [18] F.M. Leslie, *Q. J. Mech. Appl. Math.* **19**, 357 (1966).
 - [19] M. Van Dyke, *Perturbation Methods in Fluid Dynamics* (Academic, New York, 1964).
 - [20] S.A. Jewell and J.R. Sambles, *J. Appl. Phys.* **92**, 19 (2002).
 - [21] M.H. Lu, K.A. Crandall, and C. Rosenblatt, *Phys. Rev. Lett.* **68**, 3575 (1992).
 - [22] K. Okano, *Jpn. J. Appl. Phys., Part 2* **25**, L846 (1986).
 - [23] P. Bos, *Mol. Cryst. Liq. Cryst.* **114**, 329 (1984).